A Physically Based Large Signal HBT Model with Self Heating and Transit Time Effects

P. Chris Grossman
TRW Electronic Systems Group
M5 / 1464A
One Space Park
Redondo Beach, Ca 90286
(213) 814-2862
(213) 545-8479

Abstract:

A physically based, time dependent, large signal HBT model is presented which accounts for the time dependence of base, collector, and emitter charging, and includes self heating effects. The model tracks device performance over eight decades of current. The model can be used as the basis of SPICE model approximations. A thesis for the divergence of high frequency large signal SPICE simulations from measured data is presented. A new empirical equation for base-collector capacitance is included.

Introduction

Heterojunction Bipolar Transistors, HBTs, are now being used in a wide variety of both analog and digital circuits. The ability to create on chip inductors and microstrip structures on the semi-insulating substrate of $GaAl_XAs_{1-X}$ devices is ideal for microwave applications.

Accurate prediction of large signal circuit performance requires a model that is valid for a wide range of operating biases and frequencies. Existing SPICE[1] models, which are based on the Gummel-Poon model[2], do not address all effects which are key to the prediction of large signal performance of HBTs. These effects include the time dependence of the base and base-collector space charge region transit charge, multiple regions of increasing current gain, and the effects of device self heating.

A physically based, time dependent, large signal HBT model (*figures* 1 & 2) is presented which accounts for the time dependence of base, collector, and emitter charging, includes self heating effects, and accounts for the bias dependence of current gain over at least eight decades of current. The model elements are scalable with device dimensions. In addition the model may be approximated, for frequencies much less than f_t, with SPICE based simulators by assembling stock elements into macomodels (*figure* 3). The model easily reduces to the small signal hybrid π model. S. Maas[3] has shown that the DC components of the model accurately predict IM distortion at 50 MHz.

The Model

The large signal model (*figure* 1) is made up of diodes, resistors, voltage dependent capacitors, and time dependent current sources. Included is an associated thermal circuit model[5] (*figure* 2) that dynamically modifies the electrical model elements. Inherent to this model is the assumption that all of the components of the device can by modeled with independent elements. This is not strictly true since there physical interactions which couple the elements. Fortunately, these interactions comprise second order effects.

This model differs from the Gummel-Poon model used in SPICE based simulators in several ways. First, the time dependence of the base charging is accounted for, not assumed to be instantaneous as in the Gummel-Poon model. Second, all components of base current are accounted for separately, thus allowing current gain matching over many more decades of current. Third, because of the high doped base of most HBTs, conductivity modulation is ignored. Fourth, the effects of the localized (*figure* 4) self heating is included since it is not negligible.

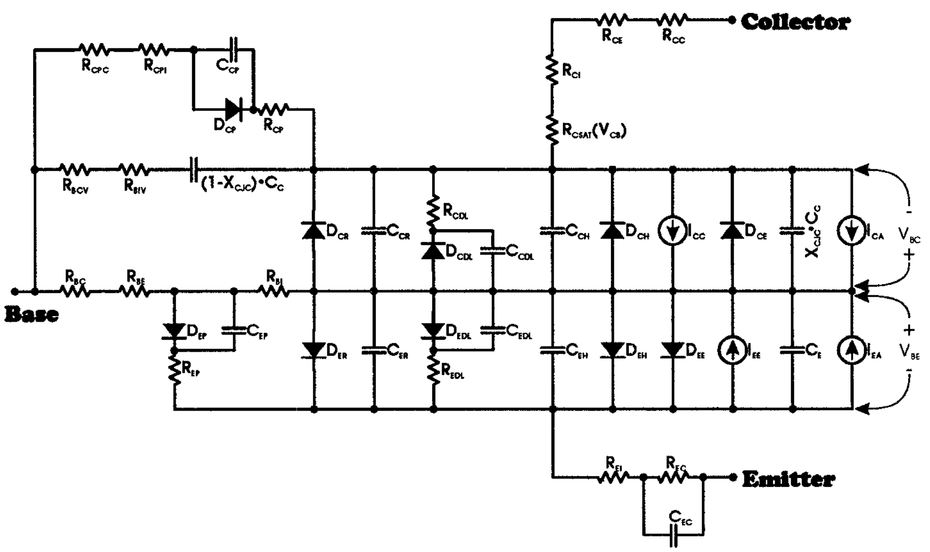

figure 1 - The schematic diagram of the electrical portion of the large signal model. V_{BE} is the voltage accross the base-emiiter space charge region, not the external device terminals. Likwise V_{BC} is the voltage accross the base-collector space charge region.

1991 IEEE MTT-S Digest

Fifth, the base-collector depletion capacitance equations account for the effects of the collector contact layer.

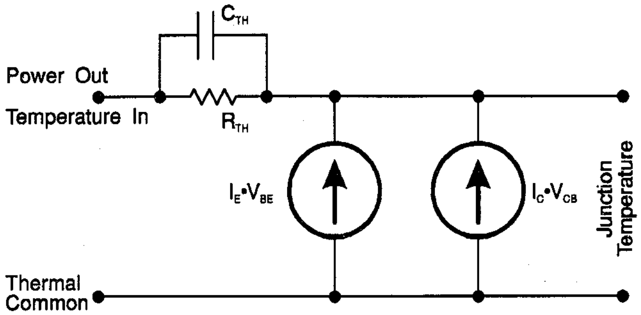

***figure* 2** - The schematic diagram of the thermal circuit. Separate power sources are provided for the base-emitter and base-collector space charge regions. When a device is in soft saturation, $I_C>0$ and $V_{CB}<0$, the base-collector region removes heat from the device. Thermal resistance between the two regions as well as power dissipation in resistors is ignored for simplicity. R_{TH} is the localized thermal resistance of the device. C_{TH} is adjusted to account for the local thermal time constant.

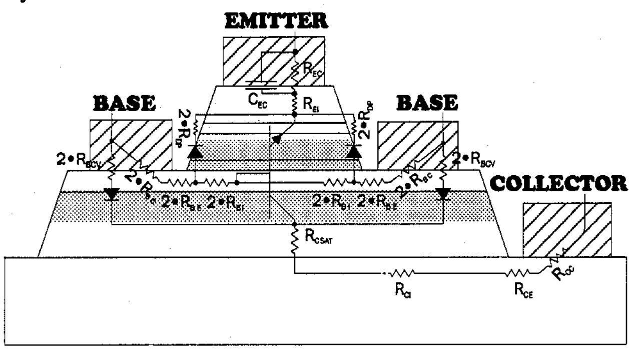

***figure* 3** - The SPICE macro model imposed on the HBT device structure.

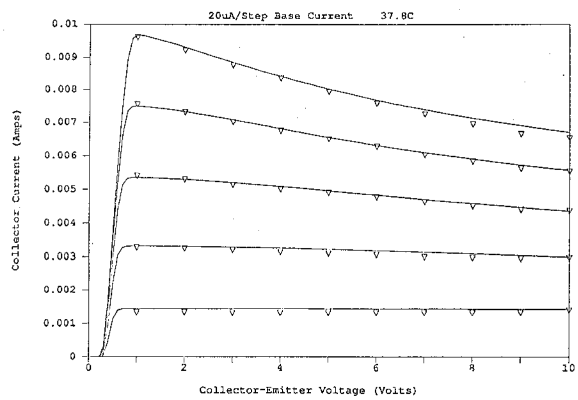

***figure* 4** - Simulated vs measured I_C/V_{CE} characteristics of a 3×10 micron TRW $GaAl_xAs_{1-x}$ HBT. The base is driven by a current source, and the collector with a voltage source. The triangles are the measured values.

The electrical model consists of diodes to model injection and recombination mechanisms, resistors, real resistors and resistors to model recombination limiting mechanisms, voltage dependent capacitors to model non transit related charge storage, and current sources to represent breakdown mechanisms and the time dependent collection of electrons from the neutral base.

R_{BC}, R_{CC}, and R_{CPC} are lateral contact resistances. R_{BI} and R_{CI} are spreading resistances. R_{BE}, R_{CPI}, R_{CE}, R_{CSAT}, and R_{EI} are simple bulk resistors. R_{CP}, R_{EP}, R_{CDL}, and R_{EDL} are resistors that model recombination limiting mechanisms.

C_E and C_C are the junction capacitances of the base-emitter and base-collector junctions respectively. C_{EP}, C_{ER}, C_{EDL}, C_{CP}, C_{CR}, and C_{CDL} are voltage dependent capacitors that model the charge storage associated with the diodes of identical subscripts. C_{EC} is the schottky junction capacitance of the emitter contact.

The base-emitter diode, D_{EE}, models the injection of electrons from the emitter into the base. D_{ER} models the optical recombination of electrons in the base-emitter space charge region (*figure* 5). D_{EP} models the base-emitter space charge region perimeter recombination. D_{EH}, which models the injection of holes into the emitter, is usually ignored because the heterojunction emitter normally prevents any significant hole injection. D_{EDL}, which models recombination through deep levels in the base-emitter space charge region, is also usually neglected.

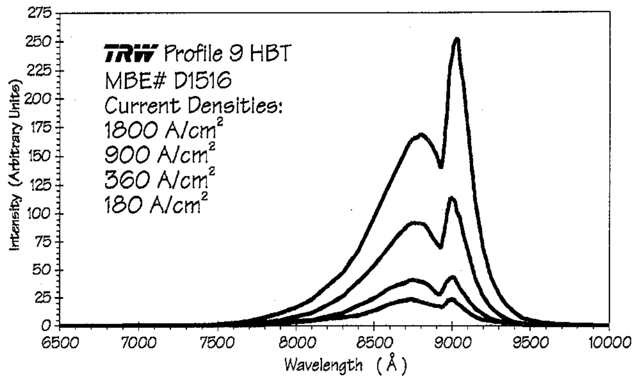

***figure* 5** - The electroluminescent emission spectra from a from a forward biased, TRW GaAlAs HBT at four collector current densities. The sharp peak at 9050Å is due to recombination in the quasi-neutral base layer. The broad peak at 8800Å is due to recombination in the base-emitter space charge layer.

The base-collector diodes D_{CE}, D_{CR}, D_{CP}, D_{CH}, and D_{EDL} are directly analogous to the above base-emitter diodes.

Current sources I_{CA} and I_{EA} provide the additional current created by avalanche breakdown in the base-collector and base-emitter space charge regions.

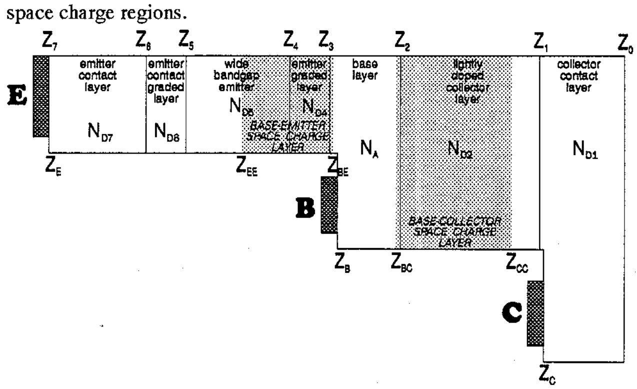

***figure* 6** - HBT layer definitions. The Zs with numerical subscripts are vertical position of the layers as grown. Z_{EE}, Z_{BE}, Z_{BC}, and Z_{CC} are the edges of the two space charge regions. After etching, Z_E is the top of the emitter mesa, Z_B is the top of the base mesa, and Z_C is the top of the substrate.

Recombination in the neutral base (*figures* 5&6) is modeled by the time dependent electron collection current sources, I_{CC} and I_{EE}. I_{CC} only collects a portion, α_F, of the injected electron current, I_F. The remainder of the current, $(1-\alpha_F)I_F$, is the portion of the base current that accounts for recombination in the neutral base region. α_F is the base transport efficiency, not the product of base transport efficiency and emitter injection efficiency as in the Ebers-Moll model.

$$I_F(t) = I_{SF} \left[\exp\left[\frac{V_{BE}(t)}{N_F V_T}\right] - 1 \right] \qquad [1]$$

The Ramo-Schockley theorem[4] requires that the collected electron current, I_{CC}, be the spatial average of the current in the base-collector space charge region (*figure* 6).

$$I_{CC} = \frac{1}{Z_{CC} - Z_{BC}} \int_{Z_{BC}}^{Z_{CC}} I(z)\, dz \qquad [2]$$

If a dual constant electron velocity profile (*figure* 7) is used to approximate the actual electron velocity profile in the base-collector space charge region, then the collected electron current, I_{CC}, can be expressed as time integral, where τ_B and τ_C are the base and total base-collector space charge region transit times. τ_{OV} is the ballistic region transit time and V_{AF} is the forward Early voltage.

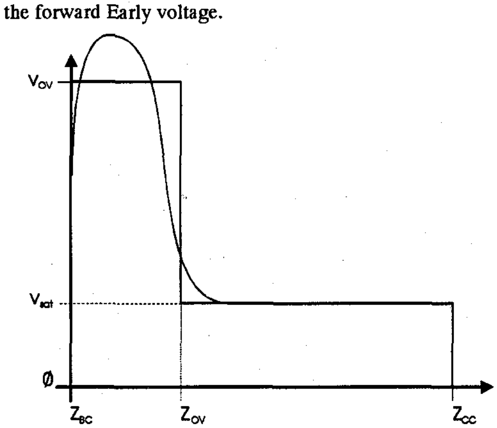

***figure* 7** - A typical electron velocity profile, for a GaAs collector, and the two region linear approximation.

The resultant base charging current, I_{QBF}, is the difference of the portion of the injected electron current, $\alpha_F I_F$, that will be collected and the collected electron current, I_{CC}.

$$W_C = Z_{CC} - Z_{BC} = \tau_{OV} v_{OV} + (\tau_C - \tau_{OV}) v_{SAT} \qquad [3]$$

$$I_{CZ}(\tau) = \alpha_F \left[1 - \frac{V_{BC}(\tau + \tau_B)}{V_{AF}} \right] I_{SF} \left[\exp\left[\frac{V_{BE}(\tau)}{N_F V_T}\right] - 1 \right] \qquad [4]$$

$$I_{CC}(t) = \frac{1}{W_C} \left[v_{OV} \int_{t - \tau_B - \tau_{OV}}^{t - \tau_B} I_{CZ}(\tau)\, d\tau + v_{SAT} \int_{t - \tau_B - \tau_C}^{t - \tau_B - \tau_{OV}} I_{CZ}(\tau)\, d\tau \right] \qquad [5]$$

$$I_{QBF}(t) = \alpha_F I_F(t) - I_{CC}(t) \qquad [6]$$

Consider now an ideal device model (*figure* 1) in which all of the resistors and all of the capacitors are of zero value, there are no breakdown effects, and the Early voltage, V_{AF}, is infinite. With the base-collector junction reverse biased a voltage step is placed across the base-emitter junction at time $t = 0$. The step response of the base charging current, I_{QBF}, the stored base charge, Q_{BF}, and the collected electron I_{CC} are shown in *figure* 9. The current and stored charge reach their steady state values once the electrons have completely traversed the base-collector space charge region at $t = \tau_B + \tau_C$.

$$Q_{BF} = \int_{t - \tau_B - \tau_C}^{t} I_{QBF}\, dt \qquad [7]$$

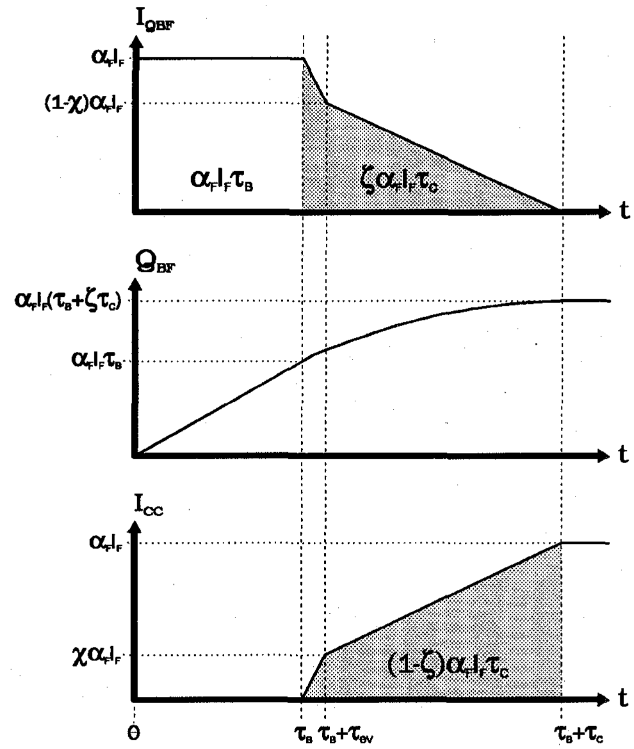

***figure* 8** - The step response of the HBT model with all resistors and capacitors set to zero. A voltage step is applied to the base-emitter junction, and the base-collector junction is reverse biased. Q_{BF} is the charge stored in the base. I_{QB} is the base charging current. I_{CC} is the collector current due to electrons collected be the base-collector space charge region.

The Gummel-Poon model as implemented in SPICE[1] assumes that this base charge changes instantaneously with the applied bias V_{BE}. It may be seen from the above analysis that this assumption is a low frequency approximation of what actually happens. This is the reason large signal simulations, with frequency components approaching $\frac{1}{2\pi(\tau_B + \tau_C)}$ using SPICE do not usually match the measured data, even when all of the passive parasitic elements have been accounted for.

In SPICE, this portion of the base charge is approximated using the quasi-steady state approximation, where τ_F is the forward transit time.

$$I_C = \alpha_F I_F \qquad [8]$$

$$Q_{BF} = I_C \tau_F \qquad [9]$$

$$\tau_F = \tau_B + \zeta \tau_C \qquad [10]$$

Assuming a quasi static base charge model, as in SPICE, $I_C \tau_B$ is the portion of the base charge needed to compensate for electrons traversing the base. $I_C \zeta \tau_C$ is the potion of the charge supplied to the base to compensate the electrons traversing the base-collector space charge region.

The remaining compensation charge for the electrons traversing the base-collector space charge region, $I_C\,(1-\zeta)\,\tau_C$ (*figure* 9) is supplied to the collector side of the region. The time dependence of the current source I_{CC} accounts for this charge automatically. The quasi static SPICE model ignores this charge stored in the collector.

Thermal Effects

Each of the diodes in the model[7] (figure 1) is described by a diode equation, equation 1 for example. The temperature dependence of the saturation current, I_{SF}, of equation 1 is described by the following equation where $I_{SF\infty}$ and T_{SF} are constants.

$$\ln(I_{SF}) = \ln(I_{SF\infty}) - \frac{T_{SF}}{T} \qquad [11]$$

The ideality factors of the diodes modeling injection, D_{EE}, D_{CE}, D_{EH}, D_{CH} are invariant with temperature. The diodes the model base-emitter heterojunction recombination, D_{ER}, D_{EP}, and D_{EDL}, have temperature dependent ideality factors. The diodes that model base-collector homojunction recombination, D_{CR}, D_{CP}, and D_{CDL}, have temperature invariant ideality factors.

In general, a simple second order Taylor approximation is used to describe the ideality factor temperature dependance. However in most cases a linear approximation will suffice. For example, the ideality factor of the base-emitter space charge optical recombination, N_{ER}, may described by the following equation with the second order term, β_{ER}, set to zero.

$$N_{ER}(T) = N_{ER}(T_0)\left[1 + \alpha_{ER}\,\Delta T + \beta_{ER}\,\Delta T^2\right] \qquad [12]$$

For temperature effects simulations, all elements of the electrical model (*figure 1*) are modified by the temperature output of the thermal subcircuit (*figure 2*).

The local thermal resistance, R_{TH} (*figure* 2), of a 3×10 micron emitter $GaAl_XAs_{1-X}$ HBT on a GaAs substrate, at 25°C, is about $900\,\frac{°C}{Watt}$. The self heating time constant, $R_{TH} \bullet C_{TH}$, is about 1 μsec. The area of self heating[5,6] is confined to within a radius of 30 microns of the junction. Thus there is little short term thermal crosstalk between devices.

This large thermal resistance has severe consequences on device operation. For a typical device with a V_{CE} of 5 Volts and a I_C of 5 mA a temperature rise of 22.5°C above the substrate temperature will occur. Given that V_{BE} changes about $\frac{-1.4\text{ mV}}{°C}$. This means that the V_{BE} of the device has decreased 31.5 mV. If this transistor were one half of the differential pair in a comparator the worst case thermal offset would be 63mV. The exact thermal offset depends on the duty cycle and frequency of the input.

The characteristic I_C/V_{CE} curves of an HBT with the apparent negative output impedance is also due to thermal effects. When the base is driven by a current source, as on a curve tracer, the slope of the output curve is entirely due to changes in DC current gain since the Early voltage, V_{AF}, is usually greater 1000 V. For most HBTs the current gain decreases as temperature increases. Thus as the device power dissipation increases, the gain drops. Simulated versus measured I_C/V_{CE} curves are shown in figure 4.

Base-Collector Junction Capacitance

The base layer (figure 6) of an HBT is typically made up of a single very highly doped layer. The collector is typically made up of two distinct layers called the lightly doped collector layer and the collector contact layer.

The base layer of an HBT is typically doped orders of magnitude higher than the lightly doped collector layer. Thus as the reverse bias on the base-collector space charge layer is increased, it will expand almost entirely in the lightly doped collector region. This will increase until the space charge layer runs into the collector contact layer.

The capacitance in each of this regions can be calculated by standard electrostatic methods. However the transition between the two regions is not as abrupt as a simple analysis would imply. The following equation may be used to fit the actual capacitance versus voltage curve of a real device. The equation is made up of two standard junction capacitance equations, one for each region, combined with a empirical factor, N_{CB}, which is adjusted for best fit to the measured data. Typically N_{CB} will range from 6 to 9. The results can be seen in *figure* 10.

$$C_C = \left[\left(\frac{C_{JC}}{\left[1-\frac{V_{BC}}{V_{JC}}\right]^{M_{JC}}}\right)^{N_{CB}} + \left(\frac{C_{JC2}}{\left[1-\frac{V_{BC}}{V_{JC2}}\right]^{M_{JC2}}}\right)^{N_{CB}}\right]^{\frac{1}{N_{CB}}} \qquad [13]$$

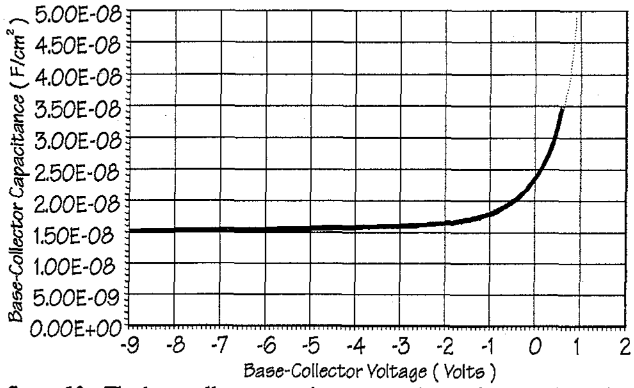

figure 10 - The base-collector capacitance per unit area for a TRW, profile 9, GaAlAs HBT. The solid curve is the measured capacitance. The dotted curve is the calculated capacitance with N_{CB} adjusted for best fit.

Conclusion

The physically based large signal model has been presented. It includes the effects of self heating, carrier transit, and a new equation for base-collector capacitance. Future large signal simulations, including distortion prediction, of HBT circuits should be improved when the full model is implemented as part of a circuit simulator. This work still remains.

Bibliography

[1] P. Antognetti and G. Massobrio, "Semiconductor Device Modeling with SPICE," McGraw-Hill, New York, 1988.

[2] H. K. Gummel and H. C. Poon, "An Integral Charge Control Model of Bipolar Transistors," *Bell System Technical Journal*, Vol. **49**, pp. 827-852, May-June 1970.

[3] Stephen A. Mass, 1990 Progress Report to TRW.

[4] Z. Djurić, M Smiljanić, and B. Radjenović, "The Application of Ramo's Theorem to Impulse Response Calculation of a Reach-Through Avalanche Photodiode," *Solid-State Electronics*, Vol. **27**(10), pp. 833-835, 1984.

[5] P. R. Strickland, "The Thermal Equivalent Circuit of a Transistor," *IBM Journal*, Vol. 3(1), pp. 35-45, April 1959.

[6] R. T. Dennison and K. M. Walter, "Local Thermal Effects in High Performance Bipolar Devices/Circuits," *Proceedings of the 1989 IEEE Bipolar Circuits and Technology Meeting*, pp. 164-167, September 1989.

[7] P. Chris Grossman and A. Oki, "A Large Signal DC Model for $GaAs/Ga_XAl_{1-X}As$ Heterojunction Bipolar Transistors," *Proceedings of the 1989 IEEE Bipolar Circuits and Technology Meeting*, pp. 258-262, September 1989.